COBEM 2025
28TH INTERNATIONAL CONGRESS OF MECHANICAL ENGINEERING

ABCM
Brazilian Society of Mechanical Sciences and Engineering
28th ABCM International Congress of Mechanical Engineering
November 09-14, 2025, Curitiba-PR, Brazil

# COB-2025-0526
# INFLUENCE OF THE EXTERNAL NOZZLE FACE PLANNING ON THE FLUID DYNAMIC BEHAVIOR AND METAL BUILDUP AT THE LANCE TIP IN LD CONVERTERS.

**João Filipe Calatrone Albuquerque Filho**
**Gabriell Rodrigues de Souza**
**Renato do Nascimento Siqueira**
**João Paulo Barbosa**
**Lucas Henrique Pagoto Deoclecio**
GPMF, Department of Mechanical Engineering, Federal Institute of Espírito Santo – Campus São Mateus, Rod. BR 101 norte, km 58, Litorâneo, São Mateus, ES, 29932-540, Brazil.
jfilipe0108@gmail.com; gabriellrodrigues987@gmail.com; renatons@ifes.edu.br; jpbarbosa@ifes.edu.br; lucas.deoclecio@ifes.edu.br

**Ayrton Cavallini Zotelle**
Department of Mechanical Engineering, Celso Suckow da Fonseca Tecnology Education Federal Center (Cefet/RJ) – Campus Angra dos Reis, Rua do Areal, 522 - Parque Mambucaba, Angra dos Reis, RJ, 23953-030, Brazil.
ayrton.zotelle@cefet-rj.br

**Breno Totti Maia**
Lumar Metals - South America Rod. MG 232 - Km 09, 70, Santana do Paraíso Minas Gerais, Brasil CEP: 35.179-000, Brazil.
breno.totti@lumarmetals.com.br

**José Roberto de Oliveira**
Department of Metallurgical and Materials Engineering, Federal Institute of Espírito Santo – Campus Vitória, Av. Vitória, 1729 - Jucutuquara, Vitória - ES, 29040-780, Brazil. jroberto@ifes.edu.br.

***Abstract.*** *Steel production in LD (Linz-Donawitz) converters uses a supersonic oxygen jet, supplied by a water-cooled metal lance equipped with convergent-divergent nozzles, to reduce the carbon concentration in the molten metal bath, transforming it into steel. Usually, multi-nozzle lances are employed due to their high mixing capacity, enhancing the efficiency of the steel refining process, but the coalescence process, caused by pressure differences between the jets, induce a complex flow structure that can lead to a deposit of metal at the nozzle tip. This metal accumulation on the external face of the lance compromises the efficiency of the LD process. This study aims to analyze the influence of the geometric change (flattening) of the external face of the nozzle on the fluid-dynamic behavior of the jet and the material buildup at the lance tip in LD converters. A computational fluid dynamics (CFD) analysis under steady-state conditions was performed using Ansys Fluent software with an adaptive mesh. The $SST\ k-\omega$ turbulence model was chosen due to its effectiveness in capturing high-pressure gradients and shock-wave flows. The simulation considered a three-dimensional lance equipped with six nozzles. The results indicate that the geometric modification applied to the lance face altered the jet flow patterns, making the coalescence more intense in the modified case compared to the original configuration. Additionally, a reduction in the recirculation zones close to the external face was observed, suggesting a decrease in material buildup. The geometric modification of the nozzle face positively affected both the jet dynamics and the operational durability of the lance.*

***Keywords:*** *LD Converter, CFD analysis, Jet coalescence, Three dimensional simulation*

## 1. INTRODUCTION

The steel produced in LD converters uses a supersonic jet supplied by convergent-divergent (CD) nozzles located at the tip of a water-cooled lance to reduce the carbon concentration in the liquid bath, transforming hot metal into steel. As shown in previous studies (Li *et al.*, 2014; Li *et al.*, 2015; Feng *et al.*, 2021; Garcia *et al.*, 2023; Zotelle *et al.*, 2024), jet flow patterns are directly influenced by nozzle configuration, which plays a key role in process efficiency.

According to Li *et al.*, 2014, various efforts have been made in the past to better understand the behavior of single- and multi-jet lances. The number of nozzles influences both jet coalescence and the performance of LD converters. Lances with three to six nozzles are commonly used, aiming to increase oxygen flow rate, reduce slopping, and minimize premature wear of the refractory lining. In addition, changes in nozzle geometry directly affect jet flow patterns. Garcia *et al.*,

2023 demonstrate that even small modifications in nozzle geometry can significantly alter jet behavior. Besides geometry, operational parameters also affect the performance of the LD process. Due to process and equipment fluctuations, operating pressure often deviates from the design pressure. Therefore, a pressure ratio (NPR) of around 12 is commonly used to ensure that the pressure at the nozzle exit is higher than the ambient pressure (Li *et al.*, 2014). This condition helps reduce lance tip wear, as well as increase the length of both the supersonic region and the potential core, promoting better mixing and enhancing the overall process efficiency.

Among the parameters that can affect jet coalescence and LD converter performance is the number of nozzles. Wang *et al.*, 2010, explain that in multi-jet lances, coalescence occurs due to the interaction between the jets and the surrounding air. As the jets move away from the nozzles in a free environment, they entrain surrounding air. In the space between the jets, this air is no longer static, and the flow accelerates to balance momentum transfer. This generates a pressure difference that is lower between the jets than around them, causing the jets to deflect toward each other and coalesce.

Garajau *et al.*, 2017, identified wear as the main limitation to lance tip life in Vallourec steelmaking plants in Brazil. The CD nozzle is made of high-purity copper, which, despite its low melting point (1085°C), offers excellent thermal conductivity when water-cooled, keeping the surface temperature below 300°C. However, it operates in an extremely aggressive environment immersed in a metal-gas-slag emulsion and exposed to high temperatures. One of the main issues arises when molten metal, driven by the flow characteristics, contacts the cooled lance tip, potentially depositing and solidifying on its face. This alters the flow pattern and accelerates wear. The objective of this work is to analyze the influence of Outer Face Flattening of the Nozzle on the Fluid Dynamic Behavior of the Medium and on material accumulation at the lance tip in LD Converters.

## 2. METHODOLOGY

The methodology employed combines a three-dimensional CFD approach based on the RANS equations with adaptive mesh refinement and Schlieren-based validation. A mesh independence test, following Zotelle et al. (2024), ensured the accuracy of the numerical domain. Simulations were performed using the SST $k-\omega$ model, with detailed flow analysis based on Mach contours and velocity fields.

### 2.1 Mathematical Formulation

The analysis of the flow pattern in supersonic jets is a three-dimensional, compressible, turbulent, and steady-state problem. It can be solved using the Reynolds Averaged Navier-Stokes (RANS) model in order to obtain the pressure fields and the average velocity, with the effects of turbulent fluctuations being modeled using the Boussinesq hypothesis to reduce the computational cost. The continuity equation is given by:

$$\nabla \cdot (\rho \mathbf{u}) = 0, \tag{1}$$

where u is the average velocity vector and $\rho$ is the density of the fluid, which, for an ideal gas, is:

$$\rho = \rho_0 \left(1 + \frac{K+1}{2} Ma^2\right)^{\frac{1}{1-K}}, \tag{2}$$

$\rho_0$ is the density of the air at the reference temperature (300 K), $K = 1.4$ is the ratio between the specific heat of the air at constant pressure ($cp$) and the specific heat at constant volume ($cv$), and $Ma = |u|/c$ is the Mach number. The speed of sound is calculated for each cell in the computational domain by $c = \sqrt{KRT}$. $R = \bar{R}/M$ is the specific gas constant, $\bar{R} = 8.31$ kJ/(kmolK) is the universal gas constant for the air, M is the molecular mass of the air, and T is the temperature of the air. The momentum equation is:

$$\nabla \cdot (\rho u \otimes u) = -\nabla P + \nabla \cdot \left[(\mu + \mu_t)\left(\nabla u + \nabla u^T - \frac{2}{3}\nabla \cdot u\,\mathbf{I}\right) - \frac{2}{3}\rho k \mathbf{I}\right], \tag{3}$$

In the above equation, $P$ is the pressure field, $\mu$ and $\mu_t$ are the molecular and turbulent thermal conductivity, respectively, and $k = (u' \cdot u')/2$ is the turbulent kinetic energy. The velocity field is determined by solving the energy equation (Eq. 4) throughout the numerical domain:

$$\nabla \cdot [u(\rho E + P)] = \nabla \cdot \left[(\lambda + \lambda_t)\nabla T + \mu\left(\nabla u + \nabla u^T - \frac{2}{3}\nabla \cdot u\mathbf{I}\right) \cdot u\right], \tag{4}$$

where $E = c_p T - P/\rho + |u|^5/2$; $\lambda$ and $\lambda_t$ are the molecular and turbulent thermal conductivity, respectively.

The turbulent viscosity ($\mu_t$) and the turbulent thermal conductivity ($\lambda_t$) were obtained by applying the turbulence closure model ( Eq.5 and Eq.6 ). The SST (Shear Stress Transport) $k$–$\omega$ model is widely used in the literature to simulate supersonic flows in Laval nozzles (Li *et al.*, 2015, Hadjadj *et al.*, 2015, Yaravintelimath *et al.*, 2016, Garcia *et al.*, 2023)

and was also used in this work. The model was developed by Menter, 1994 and has hybrid characteristics that suit simulations with the most adverse pressure gradients and presence of walls, using the robust accuracy of the $k$–$\omega$ model in regions close to walls and the $k$–$\varepsilon$ model for regions of potential flow ANSYS Inc. (2024). In this model, the turbulent viscosity is given by $\mu_t = \rho\sigma_k k/\omega$, where $\sigma_k$ is a model constant, and the thermal conductivity is $\lambda_t = \lambda\mu_t/\mu$. The turbulence model equations are the turbulent kinetic energy ($k$) equation:

$$\nabla \cdot (\rho u k) = \nabla \cdot \left[ \left( \mu + \frac{\mu_t}{\sigma_k} \right) \nabla k \right] + G_k - Y_k, \tag{5}$$

and the specific dissipation rate ($\omega$) equation:

$$\nabla \cdot (\rho u \omega) = \nabla \cdot \left[ \left( \mu + \frac{\mu_t}{\sigma_\omega} \right) \nabla \omega \right] + G_\omega - Y_\omega + D_\omega. \tag{6}$$

For these equations, $\sigma_k$ and $\sigma_\omega$ are empirical constants. $G_k$ is the production of turbulent kinetic energy, $G_\omega$ is the generation of $\omega$, $Y_k$ and $Y_\omega$ the dissipation of $k$ and $\omega$ due to turbulence and $D_\omega$ represents the cross-diffusion term. The constants used ($\sigma_k$, $\sigma_\omega$, and $c_\omega$) were the default ANSYS Fluent values.

An essential description for compressible flows is how compressibility affects the dissipation rate of $k$ and $\omega$. A compressibility function, $F(M_t)$, is used to isolate the effects of compressibility in the $k$–$\omega$ SST model, so that the dissipation of $k$ becomes:

$$Y_k = \bar{Y}_k[1 + \zeta^* F(M_t)], \tag{7}$$

and the dissipation of $\omega$:

$$Y_\omega = \bar{Y}_\omega \left[ 1 - \frac{\beta_t^*}{\beta^*} \zeta^* F(M_t) \right], \tag{8}$$

where $\bar{Y}_k$ and $\bar{Y}_\omega$ are the dissipation of $k$ and $\omega$ for the incompressible case. The constants $\zeta^*$ and $\beta_t^*$ and the function $\beta^*$ are standard in ANSYS Fluent. The function of compressibility is:

$$F(M_t) = \begin{cases} 0, & if \frac{\sqrt{2k}}{c} \leq 0.25 \\ \frac{2k}{c^2} - \frac{1}{16}, & if \frac{\sqrt{2k}}{c} > 0.25 \end{cases} \tag{9}$$

It is observed that for low values of turbulent kinetic energy, the effects of compressibility are negligible, and the dissipation rate becomes $Y_k = \bar{Y}_k$ and $Y_\omega = \bar{Y}_\omega$.

### 2.2 Numerical Methods

The geometric configuration of the oxygen lance employed in this study was based on real-world converter models with a steel production capacity of 300 tons (Maia *et al.*, 2017).

The lance features six nozzles arranged in axial symmetry. For the purpose of simplifying the analyses, certain geometric approximations were made, including a flat face at the front end of the lance and a perpendicular flat surface at each nozzle. A detailed depiction of the lance geometry is provided in Figure 1. To assess the influence of nozzle geometry, Zotelle *et al.*, 2024 proposed extending the divergent section by flattening only the nozzle exit surface, as illustrated by the red lines in Fig. 1 and in Fig. 2b. In contrast, the present study adopted a complete flattening of the external face of the lance, represented by the green lines in Fig. 1 and in Fig. 2c.

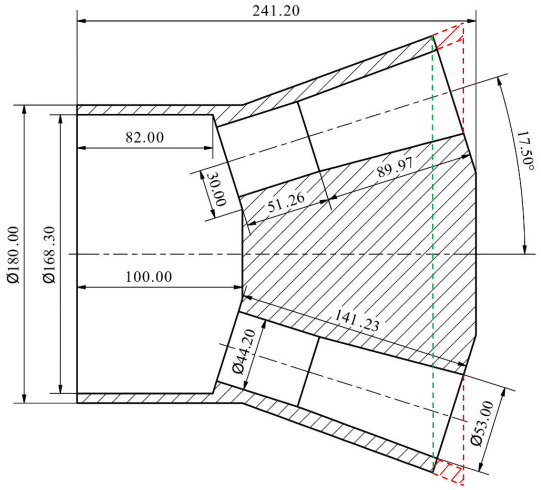


Figure 1. Mechanical technical drawing of the geometry used in LD converters and simulations. The green line represents the nozzle in the Planned External Face configuration, while the red line indicates the nozzle in the Planned Outlet configuration.

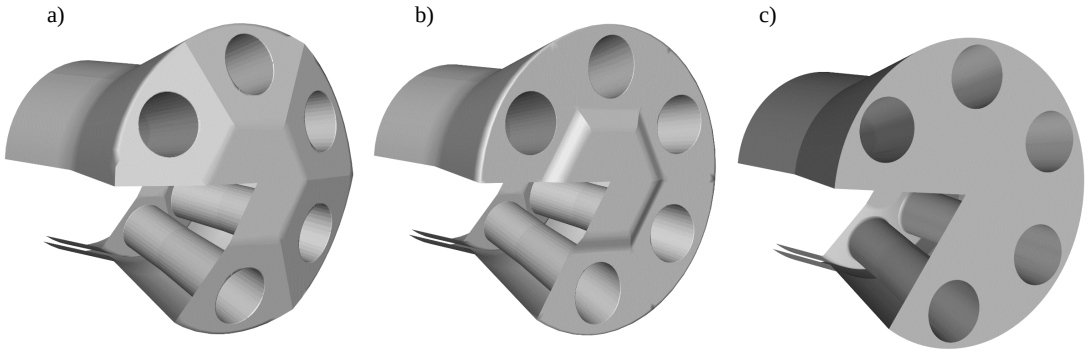


Figure 2. Configurations of the nozzles used in the simulations: a) Original, b) Planned Outlet, and c) Planned external face.

Due to the complexity of supersonic flows, simulations are often performed in two dimensional domains or under axisymmetric conditions to reduce the high computational cost associated with three-dimensional analyses (Garcia *et al.*, 2023, Igra *et al.*, 1998, and Mouronval and Hadjadj, 2005). As noted by Raje and Sinha, 2019, the interaction between multiple jets involves complex flow structures, with regimes ranging from subsonic to supersonic, and the presence of shock waves, expansion waves, and strong gradients of temperature and momentum. These flows exhibit interactions between inviscid and viscous effects, including shear layers, boundary layers, recirculation zones, and flow separation. The three-dimensional nature of the flow field induced by underexpanded jets, combined with the complex nozzle arrangement and base geometry, demands a refined computational mesh and makes CFD simulations particularly challenging. Nevertheless, three-dimensional simulations using the Reynolds-Averaged Navier-Stokes (RANS) equations remain a viable approach for predicting jet interactions, as well as pressure and heat flux distributions at the base.

For the three-dimensional simulation, in order to optimize computational cost, a 60° sector of the full geometry was used. The external domain has a length of 10,000 mm and a radius of 2,000 mm. The walls of the lance and nozzle were modeled with a no-slip condition, while the lateral surfaces (highlighted in yellow in Fig. 3) were treated as periodic, ensuring flow continuity between corresponding faces. The outer surface of the cylinder was assigned a free-slip condition, with zero gradients of tangential velocity and a normal velocity component also equal to zero.

At the inlet, an absolute pressure of 11 atm and a temperature of 300 K were prescribed, aiming for a Nozzle Pressure Ratio (NPR) of 12, a typical value in LD converter operations. The outlet was set with an absolute pressure of 0 atm

and a temperature of 300 K. Figure 3 presents the computational domain and its boundary conditions, while the nozzle geometry is detailed in Fig 1 and Fig 2c.

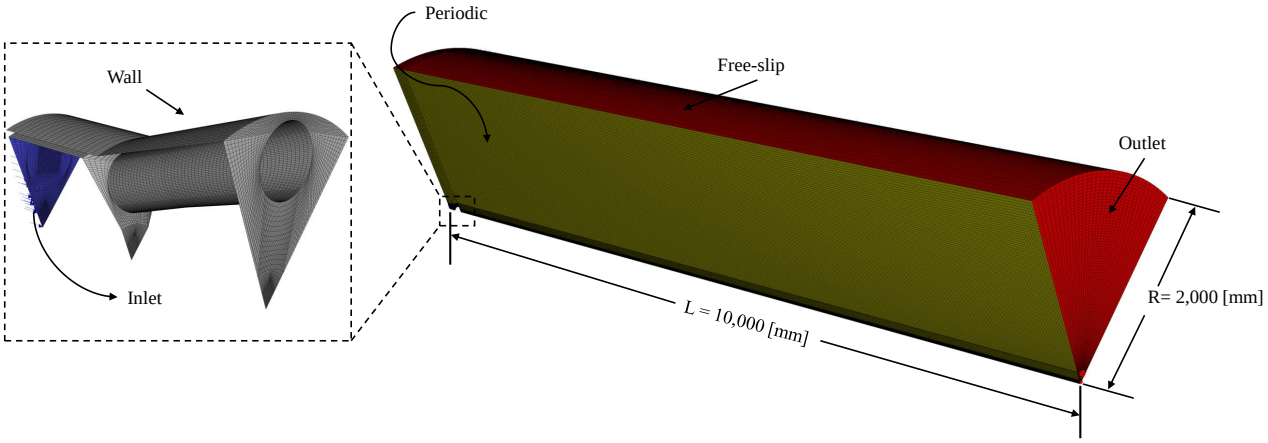


Figure 3. Numerical geometry dimensions and boundary conditions .

The mesh employed consisted of homogeneous hexahedral elements, selected for their high orthogonal quality. A coarse initial mesh was generated and subsequently refined adaptively in regions containing supersonic structures, characterized by high density gradients and Mach numbers.

The *cut-cell* method consists of subdividing the original cells into different refinement levels. In three-dimensional simulations, each cell can be divided into up to $2^{3n}$ elements, where $n$ represents the maximum level of refinement, as shown by Garcia *et al.*, 2024 and Zotelle *et al.*, 2024. Two criteria were applied to define the refined regions: cells with Mach numbers between 0.8 and 1.2 were refined in order to properly capture the supersonic core; in turn, regions with a density ratio higher than $0.5$ times the global average density were refined to more accurately represent both the potential core and the shock waves.

The simulations were performed using numerical methods based on implicit schemes, including COUPLED algorithms for pressure-velocity coupling. For spatial discretization, third-order methods were used for density and momentum, while the other methods were second-order. The simulations were carried out using the commercial CFD software Ansys FLUENT©. An overview of the fluid properties and solution methods is summarized in Table 1.

Table 1. Fluid properties and numerical methods applied to the simulations.

| | | | |
|---|---|---|---|
| **Material (Air)** | Density at ambient temperature ($\rho_0$) | | $1.225 kg/m^3$ |
| | Specific heat at constant pressure ($c_p$) | | $1006.43 J/kg{\cdot}$K |
| | Molecular viscosity ($\mu$) | | $1.7897 \times 10^{-5} Pa{\cdot}$s |
| | Molecular weight ($M$) | | $28.966 kg/kmol$ |
| | Thermal conductivity ($\lambda$) | | $0.0242 W/m{\cdot}$K |
| **Solution Methods** | Pressure-Velocity Coupling | | Coupled |
| | **Spatial Discretization** | Gradient | Least Squares Cell Based |
| | | Pressure | Second Order |
| | | Momentum | Third-order MUSCL |
| | | Density | Third-order MUSCL |
| | | Energy | Second Order Upwind |
| | | Turbulent kinetic energy ($k$) | Second Order Upwind |
| | | Specific dissipation rate ($\omega$) | Second Order Upwind |

## 3. RESULTS AND DISCUSSIONS

The initial phase of this work aimed to validate the model's ability to accurately represent the physical phenomenon, with emphasis on the supersonic structures present in three-dimensional flows through convergent-divergent nozzles. Experimental data published by Zapryagaev *et al.*, 2002, were used as a reference for comparison. Simulations of density gradient contours were performed for two different values of the nozzle pressure ratio (NPR), and the numerical results were compared with the experimental data, as shown by Garcia *et al.*, 2024 and Zotelle *et al.*, 2024. The analysis demonstrated that the numerical model was able to reproduce the jet behavior with good accuracy, thus validating it for the simulations proposed in this study.

According to Zotelle *et al.*, 2024 and Garcia *et al.*, 2024, a mesh independence test was carried out using five refinement levels ($n = 0$ to $n = 4$), based on simulations employing Schlieren images. It was observed that the initial levels ($n = 0$ and $n = 1$) did not adequately capture some flow characteristics. From level $n = 2$, the main structures began to be visualized, although some details near the nozzle exit were still not fully clear. Since levels $n = 3$ and $n = 4$ produced similar results but with a significant increase in the number of elements and, consequently, in computational cost, level $n = 3$ was adopted as the most appropriate for the simulations.

With the model validated and the appropriate mesh selected for the case under study, it was possible to carry out an analysis of the jet flow patterns. Figure 4 presents the Mach number contours for three different configurations: original, Planned outlet, and Planned external face. The results corresponding to these configurations are shown in the first, second, and third columns of the figure, respectively.

This phenomenon occurs in converging-diverging nozzles, such as those used in BOF type converters, where the pressure at the nozzle exit is higher than the ambient pressure. As a result, the jet expands immediately after exiting the nozzle. This expansion forms a protective barrier, reducing the direct impact of the flow on the nozzle surface and minimizing thermal wear. This behavior is crucial for the protection and durability of nozzles in industrial processes, such as steel refining, where high temperatures and pressures are involved. In the cases with the configuration planned external

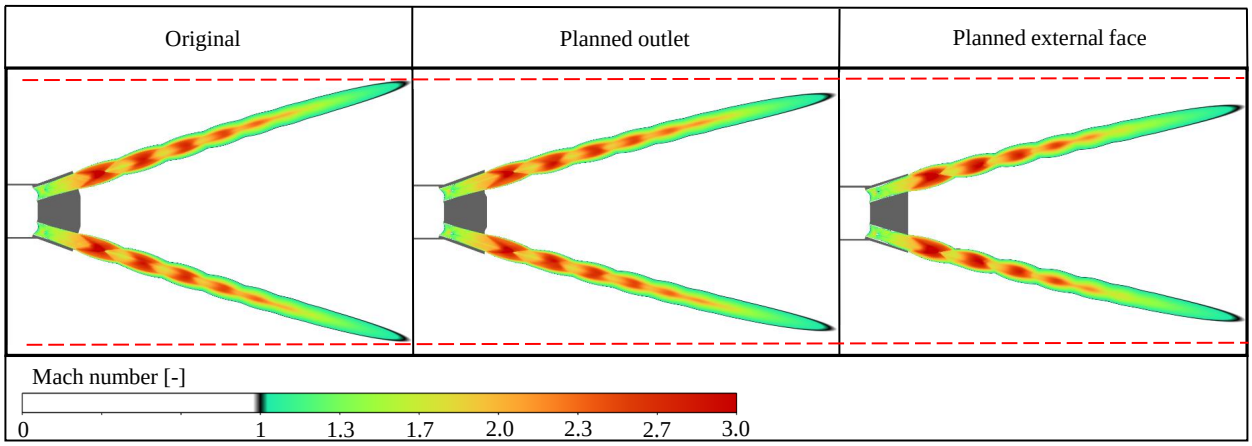


Figure 4. Supersonic core for original, Planned outlet and Planned external face configurations.

face and planned outlet, the region with the highest Mach number (indicated in red) immediately after the nozzle exit is more extensive on the inner side of the jet. This behavior indicates greater momentum in that region compared to the outer part of the jet and the original configuration. The higher velocities observed in this inner region resulted in a more intense jet coalescence, due to the momentum generated by this high velocity.

In order to deepen the analysis of the effects of geometry on jet coalescence, Fig. 5 presents the pathlines of particles initially located at the center of the nozzle exit section. For the original configuration (black line), a symmetric jet flow is observed along the same axial position, indicating a uniform flow distribution. In the Planned outlet configuration (blue line), a slight asymmetry in the jet is identified, which suggests greater coalescence compared to the original configuration. Similarly, the Planned external face configuration (red line) also exhibits asymmetry, but with the particular characteristic of displaying higher velocities immediately after the nozzle exit. This increase in velocity implies greater momentum in that region, which enhances the jet coalescence, as observed by the red dashed line on the outer side of the jets.

Figure 6 shows the density gradient contours corresponding to the three configurations analyzed. The Original configuration (Fig. 6a) exhibits an almost perfect symmetry with respect to the jet's central axis. In contrast, the Planned outlet (Fig. 6b) and Planned external face (Fig. 6c) configurations present a slight asymmetry, indicating a change in the flow behavior compared to the Original configuration.

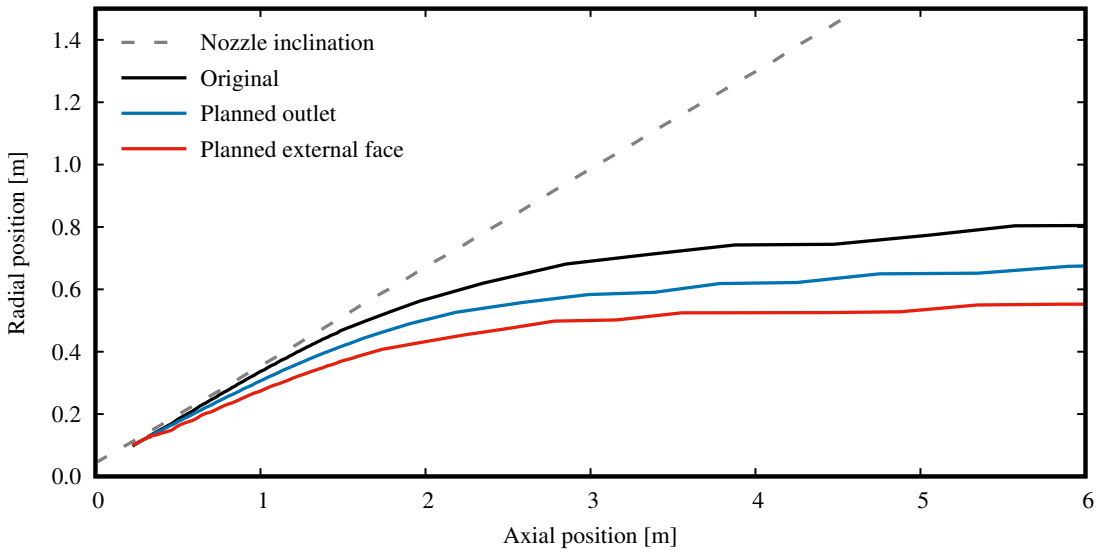


Figure 5. Influence of geometric configuration on supersonic jet coalescence for NPR 12.

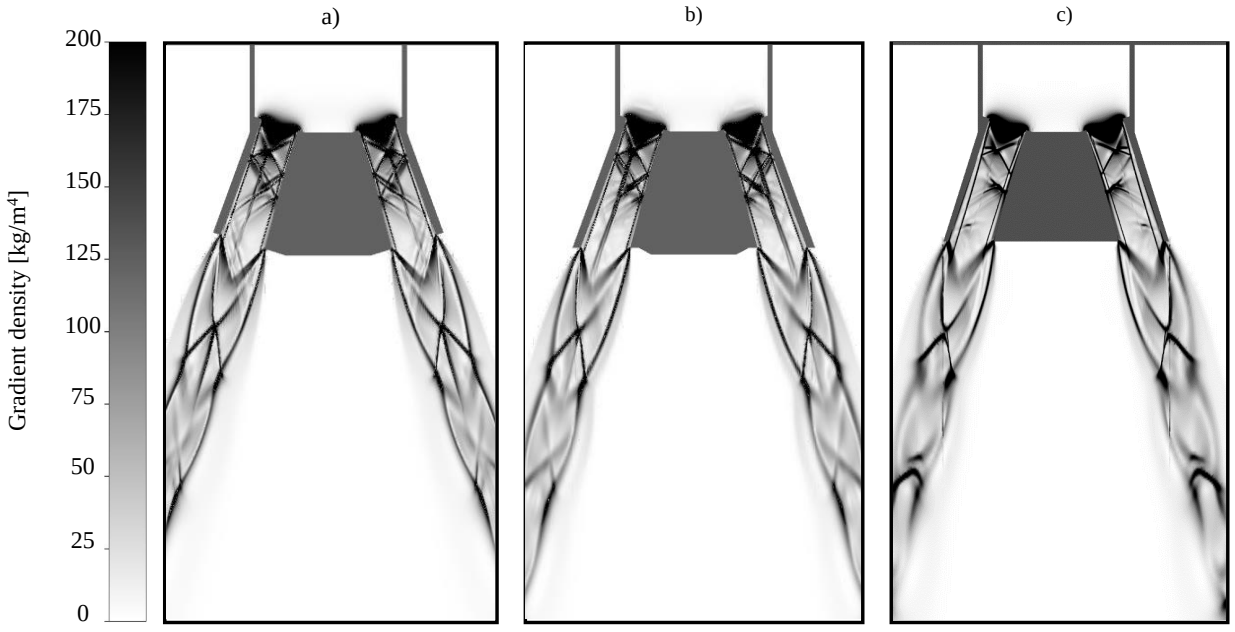


Figure 6. Density gradients for a) original, b) planned outlet, and c) planned external face configurations.

Figure 7 shows the supersonic core length for the three nozzle configurations, considering NPR = 12. Compared to the original nozzle, the configuration with a Planned Outlet presented an increase of approximately 0.86% in the supersonic core length. The configuration with the Planned External Face showed a growth of about 1.63% relative to the original, which indicates greater mixing efficiency for a given lance height.

Figure 8 presents the velocity vectors for the Original configuration (Fig. 8a), Planned Outlet (Fig. 8b), and Planned External Face (Fig. 8c). In the Original configuration, the shear zones formed by each jet, due to the drag imposed by the jets exiting the nozzles, generate a reverse flow along the lance centerline, directing the flow towards the tip of the lance. However, before reaching the tip, the flow is redirected again, moving towards the nozzle exit. The inclination of the lance face, where the nozzle exit sections are located, causes a deflection of the flow, forming a second recirculation zone of lower intensity in the central region. In this area, the flow near the lance face is convergent, meaning the jets move towards the center and, subsequently, in the middle of the front face, the flow moves away from the lance. It is worth noting that, in this configuration, the observed velocities are relatively low, not exceeding 50 m/s. where the molten metal in the emulsion can accumulate and solidify, forming a solid crust on the lance face, which compromises the performance and durability of the LD process.

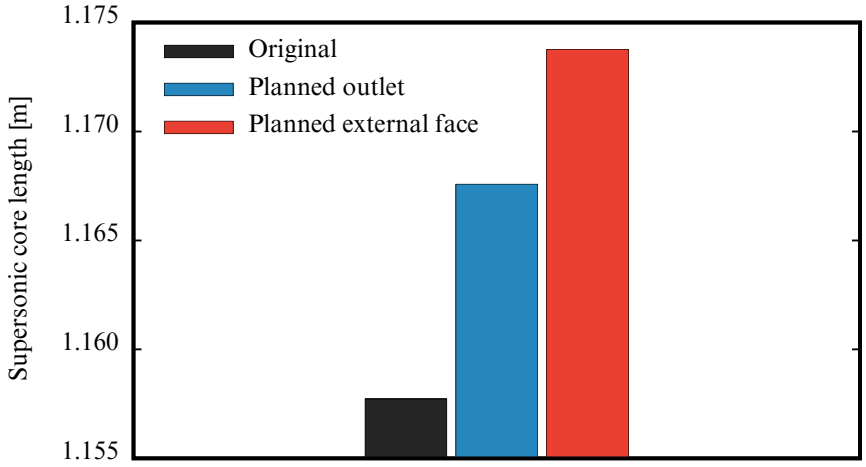


Figure 7. Influence of geometric configuration on the length of the supersonic core for NPR 12.

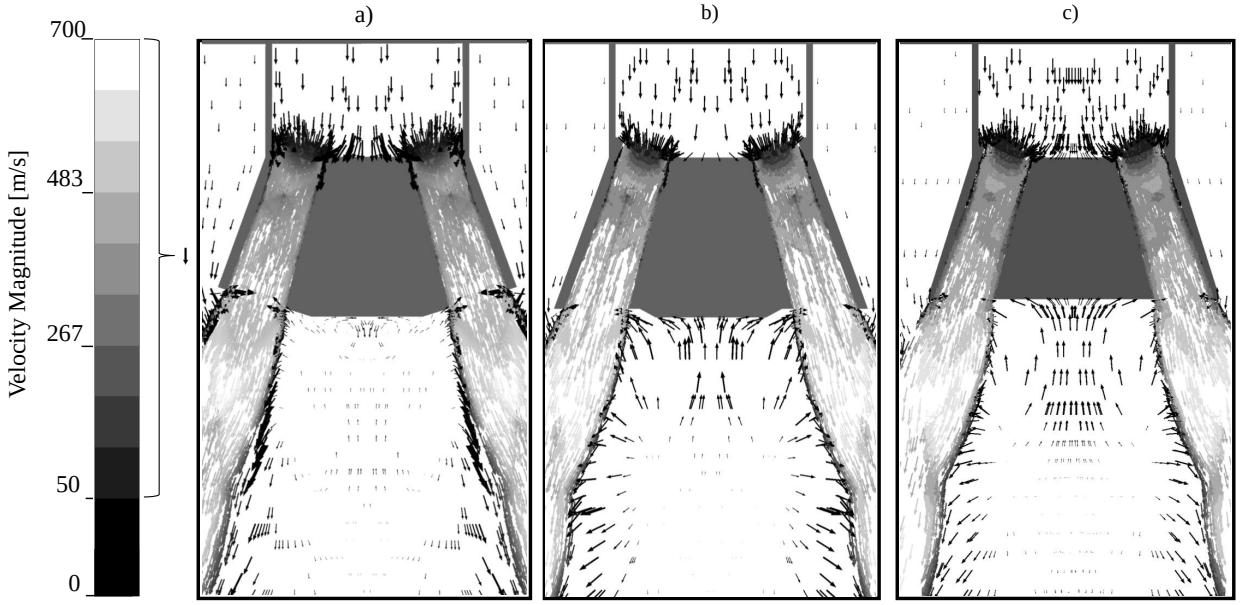


Figure 8. Velocity vectors for a) original, b) Planned Outlet and c) Planned external face configurations.

In the Planned Outlet configuration, the nozzle exit plane is positioned horizontally, altering the flow direction and eliminating the preferential direction caused by the inclination of the lance face. As a result, the reverse flow directly reaches the nozzle's front face, without the formation of the second recirculation zone. In this case, the flow direction near the lance's front face is divergent, meaning the flow moves from the center to the outer edges of the jet, which is the opposite of the direction observed in the Original configuration. This prevents the formation of a low velocity region. Moreover, for this configuration, velocity vectors exceeding 50 m/s are observed, which confirms that material accumulation will not occur in that region. The Planned External Face configuration exhibits behavior very similar to the Planned Outlet configuration. There is also no material accumulation on the lance's front face. This control over material deposition results in a significant improvement in the lance's lifespan and in the operational efficiency of the LD process.

## 4. CONCLUSIONS

The modifications made to the nozzle geometry were proposed with the aim of improving the flow pattern, increasing the service life, and facilitating the manufacturing process. With the aid of 3D numerical simulations, it was possible to analyze both the flow patterns and the indication of possible material accumulation at the lance tip, as a function of the geometric changes implemented in the nozzle. The manufacturing process of the proposed geometry was simplified, since the external face of the nozzle is completely flat. Additionally, the modifications, compared to the Planned Outlet configuration, also promoted an inversion in the direction of vortex rotation in the central region near the lance tip, which contributes to reducing the formation and accumulation of material deposits on its surface. An increase in the supersonic core length of the new nozzle was also observed, which represents a positive aspect for the process, enhancing mixing efficiency.

## 5. ACKNOWLEDGEMENTS

This work was carried out with support from Espírito Santo Research and Innovation Support Foundation (Fapes - Fundação de Amparo à Pesquisa e Inovação do Espírito Santo) –T.O. 1052/2022. The authors also thank Fapes for the grant funding that enabled this study to be conducted.

## 6. REFERENCES

ANSYS Inc., 2024. *ANSYS Fluent User's Guide*. ANSYS Inc., Canonsburg, PA, USA, release 2024r1 edition. Accessed: 2024.

Feng, C., Zhu, R., Dong, K., Wei, G., Han, B., Li, W. and Wu, W., 2021. "Effects of nozzle layout and parameters on the jet characteristics of a co 2+ o 2 mixed oxygen lance". *Metallurgical and Materials Transactions B*, Vol. 52, pp. 425–439.

Garajau, F.S., Guerra, M., Maiaa, B., Cetlinb, P. and Moreira, D.A., 2017. "Case study: Wear in supersonic nozzle of tip lance in vallourec brazil steelmaking". *AISTech 2017 Proceedings: AISTech 2017 Proceedings*, pp. 1365–1375.

Garcia, P.F., Zotelle, A.C., Siqueira, R.N., Barbosa, J.P., Maia, B.T. and Oliveira, J.R., 2023. "Numerical analysis of the effects of convergent-divergent nozzle geometry on the characteristics of supersonic jet in bof converters". In *Proceedings of the 27th International Congress of Mechanical Engineering (COBEM 2023)*. pp. 1–10.

Garcia, P.F., Zotelle, A.C., do Nascimento Siqueira, R., Barbosa, J.P., de Oliveira, J.R. and Maia, B.T., 2024. "Three-dimensional simulation of supersonic nozzle start-up structures and their consequences on the bof steelmaking process". *Proceedings of the Iron & Steel Technology Conference (AISTech 2024)*.

Hadjadj, A., Perrot, Y. and Verma, S., 2015. "Numerical study of shock/boundary layer interaction in supersonic overexpanded nozzles". *Aerospace science and technology*, Vol. 42, pp. 158–168.

Igra, O., Wang, L., Falcovitz, J. and Amann, O., 1998. "Simulation of the starting flow in a wedge–like nozzle". *Shock Waves*, Vol. 8, pp. 235–242.

Li, M., Li, Q., Kuang, S. and Zou, Z., 2015. "Coalescence characteristics of supersonic jets from multi-nozzle oxygen lance in steelmaking bof". *Steel research international*, Vol. 86, No. 12, pp. 1517–1529.

Li, M., Li, Q., Li, L., He, Y. and Zou, Z., 2014. "Effect of operation parameters on supersonic jet behaviour of bof six-nozzle oxygen lance". *Ironmaking & Steelmaking*, Vol. 41, No. 9, pp. 699–709.

Maia, B.T., Martins, A.A. and Nascimento, R.R., 2017. "Analysis of geometrical aspects of bof converters and correlations with process parameters". *Revista Matéria*, Vol. 28, No. 1, p. e13865.

Menter, F.R., 1994. "Two-equation eddy-viscosity turbulence models for engineering applications". *AIAA journal*, Vol. 32, No. 8, pp. 1598–1605.

Mouronval, A.S. and Hadjadj, A., 2005. "Numerical study of the starting process in a supersonic nozzle". *Journal of propulsion and power*, Vol. 21, No. 2, pp. 374–378.

Raje, P.V. and Sinha, K., 2019. "Three-dimensional simulation of rocket nozzles with multi-jet interaction using shock-unsteadiness model". In *AIAA Aviation 2019 Forum*. p. 3322.

Wang, W., Yuan, Z., Matsuura, H., Zhao, H., Dai, C. and Tsukihashi, F., 2010. "Three-dimensional compressible flow simulation of top-blown multiple jets in converter". *ISIJ international*, Vol. 50, No. 4, pp. 491–500.

Yaravintelimath, A., Raghunandan, B. and Moríñigo, J.A., 2016. "Numerical prediction of nozzle flow separation: Issue of turbulence modeling". *Aerospace Science and Technology*, Vol. 50, pp. 31–43.

Zapryagaev, V.I., Kudryavtsev, A.N., Lokotko, A.V., Solotchin, A.V. and Hadjadj, A., 2002. "An experimental and numerical study of a supersonic-jet shock-wave structure". *NASA STI/Recon Technical Report N*, Vol. 3, p. 12803.

Zotelle, A.C., Garcia, P.F., do Nascimento Siqueira, R., Barbosa, J.P., de Oliveira, J.R. and Maia, B.T., 2024. "Influence of geometry on flow patterns and metal accumulation at the lance tip in bof converters". In *AISTech 2024 - Proceedings of the Iron & Steel Technology Conference*. Association for Iron & Steel Technology, Columbus, Ohio, USA, pp. 624–635. doi:10.33313/388/065.

## 7. RESPONSIBILITY NOTICE

The authors are the only responsible for the printed material included in this paper